Journal of the Korean Nuclear Society
Volume 34, Number 6, pp.553~565, December, 2002

Robust Controller with Adaptation within the Boundary Layer : Application to Nuclear Underwater Inspection Robot

Gee Yong Park, Ji Sup Yoon, Dong Hee Hong, and Jae Hoo Jeong
Korea Atomic Energy Research Institute
150 Dukjin-dong, Yuseung-gu, Daejeon 305-353, Korea
gypark@kaeri.re.kr

(Receved June 12, 2002)

Abstract

In this paper, the robust control scheme with the improved control performance within the boundary layer is proposed. In the control scheme, the robust controller based on the traditional variable structure control method is modified to have the adaptation within the boundary layer. From this controller, the width of the boundary layer where the robust control input is smoothened out can be given by an appropriate value. But the improved control performance within the boundary layer can be achieved without the so-called control chattering because the role of adaptive control is to compensate for the uncovered portions of the robust control occurred from the continuous approximation within the boundary layer. Simulation tests for circular navigation of an underwater wall-ranging robot developed for inspection of wall surfaces in the research reactor, TRIGA MARK III, confirm the performance improvement.

Notational Conventions

Vectors are written in boldface roman lower-case letters, e.g., $\mathbf{x}$ and $\mathbf{y}$. Matrices are written in upper-case roman letters, e.g., G and B. And $\|\cdot\|$ means the Euclidean norm.

Key Words : robust control, adaptive control within the boundary layer, underwater robot

1. Introduction

For controlling uncertain nonlinear systems, the variable structure controller based on the sliding mode is one of the most promising candidates. In the design of sliding mode controller (SMC), the sliding surface or switching hyper plane is selected firstly and then, the equivalent control and the high speed switching control are derived by use of the sliding surface [1][2]. The sliding mode has intrinsically the invariance property but this attractive feature diminishes when SMC is implemented in control fields because of smoothing out the control input within the boundary layer for avoiding the high-frequency control input known as control chattering. In the conventional design of the SMC, the width of the boundary layer is generally thicker than the optimal width due to the conservative setup of the switching control

gain, and this inevitably reduces the control precision around the sliding surface.

For the optimal trade off between the control precision and the control chattering in deciding the width of the boundary layer, Slotine and Coetsee [3] proposed the adaptive sliding controller, where the width of the boundary layer is varied according to the variation of the uncertainty. By use of this control method, the control chattering phenomena can be eliminated but the control performance could be degraded at the time of the magnitude-increasing variation of the uncertainty. And in this method, the bounds of all uncertainties including external disturbances are the pre-requisites that the control designer must know before configuring the SMC, which may not be easy to obtain for some complex systems to be controlled or some systems under the unexpectedly varying environments.

Elmali and Olgac [4] proposed the SMC with perturbation estimation in which the switching control gain is determined from the estimate of the so-called perturbation that encloses both the modeling uncertainties and the external disturbances. From the estimation of the perturbation, the width of the boundary layer can be reduced significantly without the control chattering but the width contraction cannot continue beyond a criterion, otherwise control chattering is generated.

In this paper, the method for resolving the troublesome consideration of trade-offs between the control chattering and the control precision is proposed. In order to implement this method, an adaptive control is introduced when feedback dynamics reside in the boundary layer. This adaptive control can circumvent the problem with the boundary layer decision, guarantee the stability, and provide the improvement of the control performance within the boundary layer for nonlinear systems with the uncertainty whose dynamics are slow. In this control scheme, the width of the boundary layer can be given by an appropriate but fully conservative value. As described later, the adaptive control in composed of the static and the dynamic adaptation gains. The dynamic gain is derived based on some restricted properties of system dynamics. From the property of the adaptation gains, this adaptive control does not activate independently but rather, keeping pace with the robust control, it compensates the undesirable effects not covered by the robust controller.

In this paper, the basic or equivalent control law is derived on the nonlinear prediction model suggested by Lu [5], which dictates the relationship of a certain future output to the current input, so that this can skip over the design of invariant hyper plane. Robust controllers based on the nonlinear prediction model for the SISO (Single Input and Single Output) system were described in Park, et al [6][7]. The control scheme presented in this paper is the MIMO (Multi-Input and Multi-Output) extension of the SISO case in Ref.[7]. For convenience, throughout this paper, the arguments t and x are sometimes omitted when no confusion is likely to arise.

2. Robust Control Law

Consider the nonlinear system represented as

$$\dot{\mathbf{x}} = \mathbf{a}(\mathbf{x}) + B(\mathbf{x})\mathbf{u}(t), \quad \mathbf{y} = \mathbf{c}(\mathbf{x}), \tag{1}$$

where $\mathbf{x} \in X \subset R^n$ is the measurable state, $\mathbf{u} \in U \subset R^m$ the control input, and $\mathbf{y} \in R^m$ the output. The functions $\mathbf{a}$, B, and $\mathbf{c}$ that have appropriate dimensions are supposed to be sufficiently smooth and have finite magnitudes, respectively. The domain X contains the origin and U is a compact set. Almost all of mechanical robot dynamics can be represented by Eq.(1), which is called the

regular form ($m \le n$).

Let r_i be the relative degree of *i*th output component. Then, Eq.(1) can be represented, more generally, by

$$\mathbf{y}^r(t) = \mathbf{f}(\mathbf{x}) + G(\mathbf{x})\mathbf{u}(t), \tag{2}$$

where $\mathbf{y}^r=[y_1^{(r_1)} \cdots y_m^{(r_m)}]^T$, $\mathbf{f}(\mathbf{x})=[L_a^{r_1}(c_1)\cdots L_a^{r_m}(c_m)]^T$, $G(\mathbf{x})$ is nonsingular, and *i*th raw vector $\mathbf{g}(\mathbf{x})=[L_{b_1}(L_a^{r_1-1}(c_i))\cdots L_{b_m}(L_a^{r_i-1}(c_i))]$. In the definitions, c_i and $\mathbf{b}_j$ are *i*th component of output function and *j*th column vector of B, respectively, and the operator L means the Lie derivative [8], for example, the Lie derivative of c_i with respect to $\mathbf{f}$ is defined as $L_f(c_i)=\frac{\partial c_i}{\partial \mathbf{x}}\mathbf{f}$ and $L_f^{r_i}(c_i)$ is the r_ith order Lie derivative of c_i to $\mathbf{f}$ represented as $L_f^{r_i}(c_i)=L_f(L_f^{r_i-1}(c_i)) = \cdots = L_f(\cdots(L_f(L_f(c_i))))$ with $L_f^0(c_i)=c_i$. In Eq.(2), the superscript r means total relative degree ($r = r_1+ \cdots +r_m$).

As suggested by Lu [5], the future system and desired outputs for time t+h (h>0) from current time t are predicted by

$$\mathbf{y}(t+h) = \mathbf{z}(t) + \Lambda(h)\left[\mathbf{f}(\mathbf{x}) + G(\mathbf{x})\mathbf{u}(t)\right], \tag{3a}$$

$$\mathbf{y}_d(t+h) = \mathbf{z}_d(t) + \Lambda(h)\mathbf{y}_d^r(t), \tag{3b}$$

where $\mathbf{y}$ and $\mathbf{y}_d$ are the system output and desired output, respectively, h is the prediction time interval, $\mathbf{y}_d^r = [y_{d,1}^{(r_1)} \cdots y_{d,m}^{(r_m)}]^T$, and $\Lambda(h)$ is the $m \times m$ diagonal matrix represented as

$$\Lambda(h) = \mathrm{diag}\left[\frac{h^{r_1}}{r_1!} \quad \frac{h^{r_2}}{r_2!} \quad \cdots \quad \frac{h^{r_m}}{r_m!}\right].$$

The each component of $\mathbf{z}$ and $\mathbf{z}_d$ are represented as

$z_i(t)=\lambda_i(h)\ \phi_i(t)$ and $z_{d,i}(t)=\lambda_i(h)\ \phi_{d,i}(t)$, (for $i=1, \cdots, m$)

where $\lambda_i(h)=\left[1, h, \cdots, \frac{h^{r_i-1}}{(r_i-1)!}\right]$, $\phi_i=[y_i, \dot{y}_i, \cdots, y_i^{(r_i-1)}]^T$, $\phi_{d,i}=[y_{d,i}, \dot{y}_{d,i}, \cdots, y_{d,i}^{(r_i-1)}]^T$, and all are the $r_i \times 1$ vector.

The future output error e(t+h) is defined as

$$\begin{aligned}\mathbf{e}(t+h) &= \mathbf{y}(t+h) - \mathbf{y}_d(t+h)\\ &= \mathbf{z}_e(t) + \Lambda(h)\mathbf{f}(\mathbf{x}) + \Lambda(h)G(\mathbf{x})\mathbf{u}(t)\\ &\quad - \Lambda(h)\mathbf{y}_d^r(t),\end{aligned} \tag{4}$$

where $\mathbf{z}_e = \mathbf{z} - \mathbf{z}_d$. The control objective for the future output error to be minimized has the form of

$$J(t+h) = \frac{1}{2}\mathbf{e}(t+h)^T\mathbf{e}(t+h). \tag{5}$$

The basic control law is produced from the fact that the control input obtained at time t should minimize the control objective at time t+h, namely, $\partial J(t+h)/\partial \mathbf{u}(t) = \mathbf{0}$. The basic control law $\mathbf{u}_c$ derived in this way, by use of Eq.(4), is as follows

$$\begin{aligned}\mathbf{u}_c(t) = &-(\Lambda(h)G(\mathbf{x}))^{-1}\\ &\left[\mathbf{z}_e(t) + \Lambda(h)\mathbf{f}(\mathbf{x}) - \Lambda(h)\mathbf{y}_d^r(t)\right].\end{aligned} \tag{6}$$

The closed loop dynamics by inserting the control input Eq.(6) into Eq.(2) are expressed as

$$\mathbf{e}^r(t) + \Lambda(h)^{-1}\mathbf{z}_e(t) = \mathbf{0}, \tag{7}$$

where $\mathbf{e}^r=[e_1^{(r_1)}\cdots e_m^{(r_m)}]^T = \mathbf{y}^r - \mathbf{y}_d^r$. The feedback dynamics in (7) are stable for $r_i \le 4$ ($i=1,\cdots,m$). As can be seen in Eq.(6) and Eq.(7), the prediction time interval h has the role of the controller gain and also determines the feedback dynamics. If $r_i>4$, the basic control law is modified such as

$$\begin{aligned}\mathbf{u}_c(t) = &-(\Lambda(h)G(\mathbf{x}))^{-1}\\ &\left[\mathbf{z}_e(t) + \Lambda(h)\mathbf{f}(\mathbf{x}) - \Lambda(h)\mathbf{y}_d^r(t) + \mathbf{v}(t)\right],\end{aligned}$$

where $\nu(t)= -\mathbf{z}_e(t)+\Lambda(h)\bar{\nu}(t)$ and *i*th component of $\bar{\nu}(t)$ is represented as $\bar{\nu}_i(t)=\lambda_{\nu,i}(h)\ \phi_{e,i}(t)$ with $\phi_{e,i}=[e_i, \dot{e}_i \cdots e_i^{(r_i-1)}]^T$. $\lambda_{\nu,i}$ is composed of appropriate coefficients,

so that the resulting feedback dynamics satisfy the Hurwitz equation.

For the case that the nonlinear system has the uncertainty that includes the modeling uncertainties and the external disturbances, the dynamic equation is represented as

$$\mathbf{y}^{r}(t) = \hat{\mathbf{f}}(\mathbf{x}) + \hat{G}(\mathbf{x})\mathbf{u}(t) + \boldsymbol{\eta}(t), \tag{8}$$

where $\boldsymbol{\eta}(t)=(\mathbf{f}(\mathbf{x}) - \hat{\mathbf{f}}(\mathbf{x}))+(G(\mathbf{x}) - \hat{G}(\mathbf{x}))\mathbf{u}+\mathbf{d}_E(t)$. $\hat{\mathbf{f}}$ and $\hat{G}$ are known functions and $\mathbf{d}_E$ represents the external disturbances. $\hat{G}$ should be nonsingular. The corresponding basic control law is

$$\mathbf{u}_c(t) = -(\Lambda(h)\hat{G}(\mathbf{x}))^{-1} \left[\mathbf{z}_e(t) + \Lambda(h)\hat{\mathbf{f}}(\mathbf{x}) - \Lambda(h)\mathbf{y}_d^{r}(t)\right] \tag{9}$$

For deriving the robust and adaptive controls, we make the following assumptions.

Assumption 1: The gross information for G and **f** are obtainable, so that the bounds for those functions can be identified in such a way that

$$\left\|\mathbf{f}(\mathbf{x}) - \hat{\mathbf{f}}(\mathbf{x})\right\| \le d_F(\mathbf{x}) \quad \text{and}$$
$$\left\|\Sigma_M\right\| = \left\|G(\mathbf{x})\hat{G}(\mathbf{x})^{-1} - I_m\right\| \le \gamma_o < 1, \text{ for all } \mathbf{x} \text{ and } t,$$

where $\Sigma_M = G\hat{G}^{-1} - I_m$, γ_o is a positive scalar value less than 1, and I_m is the m × m identity matrix.

Assumption 2: The magnitude of external disturbances can be bounded by

$$\left\|\mathbf{d}_E(\mathbf{x}, t)\right\| \le d_{EB} \quad \text{for all } \mathbf{x} \text{ and } t.$$

Assumption 3: Σ_M in Assumption 1 can be divided by its diagonal and non-diagonal terms such that $\Sigma_M=\Sigma_M^D+\Sigma_M^{ND}$ where Σ_M^D is the diagonal term and Σ_M^{ND} is the off-diagonal term. It is supposed that the magnitude of Σ_M^{ND} is reasonably smaller than 1, i.e., $\| \Sigma_M^{ND} \| \ll 1$.

Control input is now such that $\mathbf{u} = \mathbf{u}_c + \mathbf{u}_R$ where $\mathbf{u}_R$ is the robust control. The feedback dynamics with this control become

$$\mathbf{e}^{r}(t) + \Lambda(h)^{-1}\mathbf{z}_e(t) = \mathbf{u}_R^M(t) + \boldsymbol{\eta}(t), \tag{10}$$

where $\mathbf{u}_R^M = \hat{G}\mathbf{u}_R$. Eq.(10) can be further arranged by

$$\dot{\mathbf{e}}_v(t) = \Gamma_v\mathbf{e}_v(t) + B_v(\mathbf{u}_R^M(t) + \boldsymbol{\eta}(t)), \tag{11}$$

where $\mathbf{e}_v$ is the augmented error vector of $r \times 1$, Γ_v and B_v are, respectively, $r \times r$ and $r \times m$ matrices.

Define $\boldsymbol{\eta}_c=(\mathbf{f} - \hat{\mathbf{f}}) + (G - \hat{G})\mathbf{u}_c+d\mathbf{l}_E$. The magnitude of $\boldsymbol{\eta}_c$ is supposed to be bounded by $\| \boldsymbol{\eta}_c \| \le d_\eta$ in which $d_\eta=d_F(\mathbf{x})+\gamma_o \| \mathbf{d}_s(\mathbf{x}) \| +d_{EB}$ and $\mathbf{d}_s(\mathbf{x}) = -\Lambda(h)^{-1}\mathbf{z}_e - \hat{\mathbf{f}}(\mathbf{x})+\mathbf{y}_d^{r}$.

The transformed robust control $\mathbf{u}_R^M$ is defined as

$$\mathbf{u}_R^M(t) = \begin{cases} -d_{max}\dfrac{\overline{\mathbf{m}}(t)^T}{\|\overline{\mathbf{m}}(t)\|} & ;\| \overline{\mathbf{m}} \| \neq 0 \\ \mathbf{0} & ;\| \overline{\mathbf{m}} \| = 0 \end{cases}, \tag{12}$$

In (12), $\overline{\mathbf{m}}$ is called, hereafter, the error measure function and defined by $\overline{\mathbf{m}} = \mathbf{e}_v^T P B_v$ where the symmetric positive definite matrix P satisfies, for a positive definite matrix Q, the Lyapunov equation of $\Gamma^T P+P\Gamma= - Q$. The positive scalar d_{max} in Eq.(12) is given by

$$d_{max} = \frac{1}{1-\gamma_o}(d_\eta + \xi), \tag{13}$$

where ξ is a small non-negative value ($\xi \ge 0$).

At this time, we make the following proposition.

Proposition 1: Suppose the uncertain nonlinear system is represented by Eq.(8) and Assumptions 1 and 2 are valid. Then, the basic control law Eq.(9) and the robust control Eq.(12) with the switching control gain in Eq.(13) guarantee the asymptotic output tracking, i.e., $\mathbf{y}(t) \to \mathbf{y}_d(t)$ as $t \to \infty$.

Proof: See Appendix A. ■

In order to avoid the control chattering, the

transformed robust control Eq.(12) is modified as

$$\mathbf{u}_R^M(t) = \begin{cases} -d_{max}\dfrac{\overline{\mathbf{m}}(t)^T}{\|\overline{\mathbf{m}}(t)\|} & ;\|\overline{\mathbf{m}}\| \geq \varepsilon \\ -d_{max}\dfrac{\overline{\mathbf{m}}(t)^T}{\varepsilon} & ;\|\overline{\mathbf{m}}\| < \varepsilon \end{cases}, \qquad (14)$$

where ε is the boundary value that determines the width of the boundary layer.

The robust control is obtained by $\mathbf{u}_R = \hat{G}^{-1}\mathbf{u}_R^M$. With the transformed robust control Eq.(14), the asymptotic convergence of tracking error is guaranteed for only the region outside the boundary layer. The structure of the transformed robust control is changed according to the status of $\|\overline{\mathbf{m}}\|$ to the boundary value ε. With regard to this notion, $\|\overline{\mathbf{m}}\|$ is called the error measure.

3. Adaptive Control Within the Boundary Layer

The robust control derived in the previous section has continuous values by linearizing the discontinuous function within the boundary layer and thereby, the control chattering can be eliminated by just selecting the proper boundary value of ε. However, the stability and convergence of the feedback system cannot be guaranteed within the boundary layer and may be lost due to continuous approximation. Moreover, the width of boundary layer is wanted to be as small as possible for high tracking precision but is, in reality, set to a more larger value due to the conservative setting of the uncertainty bound.

In order to remove the potential instability and also improve the control performance within the boundary layer, the adaptive control is introduced. This adaptive control also provides a high tracking precision under the conservative boundary value.

In this paper, an adaptation mechanism has two distinguished features. First, the role of adaptive control is to support the robust control within the boundary layer. Second, its adaptation rule involves two adaptation gains, that is, the static adaptation gain and the dynamic adaptation gain. The static adaptation gain is a constant value as can be seen in the conventional adaptation rules. The dynamic adaptation gain is updated at every control instance and varies according to the behavior of the error measure within the boundary layer.

The error dynamics with the control input $\mathbf{u}=\mathbf{u}_c+\mathbf{u}_R+\mathbf{u}_A$ in which $\mathbf{u}_A$ is the adaptive control are represented by

$$\dot{\mathbf{e}}_v = \Gamma_v \mathbf{e}_v + B_v(\mathbf{u}_R^M + \mathbf{u}_A^M + \boldsymbol{\eta} + \mathbf{d}_E^U), \qquad (15)$$

where $\mathbf{e}_v$, Γ_v, B_v, and $\boldsymbol{\eta}$ are defined in the previous sections and $\mathbf{u}_A^M = \hat{G}\mathbf{u}_A$. In Eq.(15), as different from Eq.(11), the term $\mathbf{d}_E^U$ is included and is defined as the unexpected disturbance whose magnitude is not too large.

Define

$$\tilde{\mathbf{d}}(t) = \boldsymbol{\eta}_c^M(t) + \delta(t)^{-1}\mathbf{u}_A^M(t), \qquad (16)$$

where $\boldsymbol{\eta}_c^M = (G\hat{G}^{-1})^{-1}(\boldsymbol{\eta}_c + \delta(t)^{-1}\mathbf{d}_E^U)$ and $\delta(t)$ is called the dynamic adaptation gain with the range of $0 < \delta(t) \leq 1$ within the boundary layer. Then, we make the following proposition.

Proposition 2: Suppose again the nonlinear system Eq.(8) with the unexpected disturbance as in Eq.(15) and Assumptions 1 and 2 are valid. It is assumed that the dynamics of uncertainty are slow. If we set the adaptive updating law as

$$\dot{\tilde{\mathbf{d}}}(t) = -\delta(t)\Gamma_S(G(\mathbf{x})\hat{G}(\mathbf{x})^{-1})^T\overline{\mathbf{m}}(t)^T, \qquad (17)$$

where Γ_S is a positive definite diagonal matrix called the static adaptation gain and also set the dynamic adaptation gain by

$$\delta(t) = 1 - \frac{\|\overline{\mathbf{m}}(t)\|}{\varepsilon} \quad (\text{for } \|\overline{\mathbf{m}}(t)\| < \varepsilon), \qquad (18)$$

then, the asymptotic output tracking, $\mathbf{y}(t)\rightarrow\mathbf{y}_d(t)$ as $t\rightarrow\infty$, for feedback system inside the boundary layer can be achieved.

Proof: See Appendix B. ■

For slow dynamics of uncertainty, the adaptive updating law Eq.(17), with the assumption of the slow variation of the dynamic adaptation gain, is represented as

$$\dot{\mathbf{u}}_A^M(t) = -\delta(t)^2\Gamma_S(G(\mathbf{x})\hat{G}(\mathbf{x})^{-1})^T\overline{\mathbf{m}}(t)^T. \quad (19)$$

The assumption of the negligible dynamics of the dynamic adaptation gain is given from the fact that it can never cause any serious problem in control performance through the various control simulations. The adaptive updating law for the appropriate quantity of uncertainty is composed of two types of gains as in Eq.(19): One is the static adaptation gain Γ_S which has constant values and the other the dynamic adaptation gain $\delta(t)$ whose value is updated for every control instance. But, adaptive updating law Eq.(19) cannot be realized because its structure contains the unknown function G(x). To overcome this problem, Eq.(19) is further manipulated as follows.

$$\dot{\mathbf{u}}_A^M(t) = -\delta(t)^2\Gamma_S I_m\overline{\mathbf{m}}(t)^T - \delta(t)^2\Gamma_S(\Sigma_M)^T\overline{\mathbf{m}}(t)^T,$$

$$= -\delta(t)^2\Gamma_S\left[I_m+\Sigma_M^D\right]^T\overline{\mathbf{m}}(t)^T - \delta(t)^2\Gamma_S\left(\Sigma_M^{ND}\right)^T\overline{\mathbf{m}}(t)^T.$$

By Assumption 3, the second term in the right hand side of the above equation is much smaller than the first term and hence, the second term of the right hand side can be neglected. Moreover, by use of the fact that $\|\Sigma_M^D\| \le \|\Sigma_M\| < 1$ and $\|I_m\| \ge 1$, the terms in the bracket, $I_m+\Sigma_M^D$, are always positive definite (i.e., positive diagonal values). And thus, the effect of $I_m+\Sigma_M^D$ can be involved into the static adaptive gain Γ_s by tuning the values in this gain. Finally, the adaptive updating law is given by

$$\dot{\mathbf{u}}_A^M(t) = -\delta(t)^2\Gamma_S\overline{\mathbf{m}}(t)^T, \quad (20)$$

with the proper tuning of the static adaptation gain. Let t_b be the time when the error measure begins to enter the boundary layer and the adaptive control at this time is set to zero. Then, the adaptive control is obtained by

$$\mathbf{u}_A^M(t) = \int_{t_b}\dot{\mathbf{u}}_A^M(\tau)d\tau \quad \text{and} \quad \mathbf{u}_A(t) = \hat{G}(\mathbf{x})^{-1}\mathbf{u}_A^M(t). \quad (21)$$

Remarks:

(1) As can be seen in Appendix B, the adaptive control shares the task of the robust control that is the compensation for the undesired effects of modeling uncertainties and disturbances within the boundary layer. At the boundary layer where the value of the dynamic adaptation gain is small as in Eq.(18), the robust control takes more portion of undesired effects and hence, the adaptive control compensates small portion of these effects. As the error measure goes inside the boundary layer, the amount of the task that the adaptive control should take increases and finally, the adaptive control takes almost amount of the task at points very close to zero of the tracking error.

(2) As in Eqs.(15) and (16), the unexpected disturbance is included in deriving the adaptive control and this effect is not reflected in the robust control. The adaptive control can compensate the effect of the unexpected uncertainty that affects the system whose error measure resides within the boundary layer. It is noted that the unexpected disturbances can only be manipulated within the boundary layer. For reducing the damage of the unexpected disturbances at the outside of the boundary layer, some useful methods could be configured: First, the bounded values of the modeling uncertainties and the external disturbances are set to sufficiently large values, respectively, which will obviously demand the large control authority. In order to reduce the undesired

effects of the large control authority, the boundary value is given to a large value so that the reaching time of the error dynamics onto the boundary layer could be shortened. At the boundary layer, the value for the uncertainty bound is changed into the minimum estimated value and the adaptive control is activated for compensating all undesired effects. Second, this control method is incorporated with the control method proposed by Yoo and Chung [9] or Elmali and Olgac [4], where the switching control gain is updated by on-line uncertainty bound estimation.

(3) With the adaptive control, it is expected that high tracking precision can be achieved under the more conservative boundary value. This means the control designer may set the boundary value to a relatively large one just for avoidance of the control chattering without concerning about the degradation of the high control precision.

5. Simulations

The controller described in the previous sections is applied to the motion control of an underwater wall-ranging robot (UWR) that was developed for the inspection of the contaminated level on the surfaces of inner wall and bottom in the nuclear research reactor, TRIGA MARK III [10][11]. Fig.1 shows the UWR fabricated. This UWR is designed to navigate autonomously on the wall surfaces and within the water pool. Operational procedure of UWR in the nuclear research reactor is depicted in Fig.2. Detailed descriptions of this UWR are presented in Ref.[10] and Ref.[11].

Fig.3 shows the two coordinate systems for UWR, i.e., the global coordinate defined by (X, Y, ϕ) and the local coordinate by (x, y, ϕ). The dynamic motion for UWR is described by

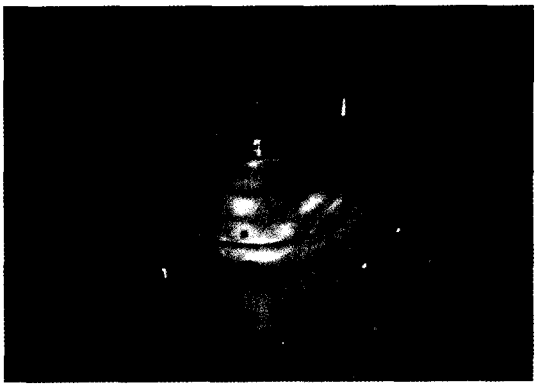

Fig. 1. Underwater Wall-Ranging Robot

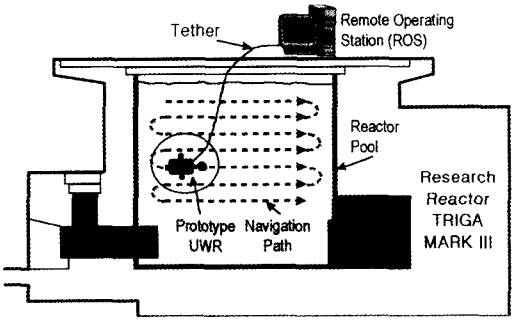

Fig. 2. Inspection Procedure of UWR

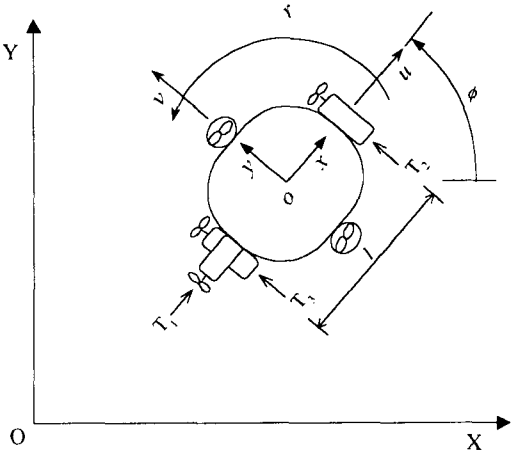

Fig.3. Global and Local Coordinates of UWR

$$\ddot{\mathbf{x}} = \mathbf{M}_t^{-1}\mathbf{f}_M(\mathbf{x},\dot{\mathbf{x}}) + \mathbf{M}_t^{-1}\mathbf{u}_I, \tag{22}$$

where $\mathbf{x}$ is the state vector such that $\mathbf{x} = [x_1\ x_2\ x_3]^T = [x\ y\ \phi]^T$ (ϕ is called the yaw or heading angle), M_t is the total mass (the sum of the robot mass and the added mass) and $\mathbf{f}_M$ includes all resistive forces (including drag forces), and $\mathbf{u}_I$ is control input given by resultant thrust forces. The outputs of UWR are its state vector (x, y, ϕ): the position and the direction of UWR. M_t, $\mathbf{f}_M$, and $\mathbf{u}_I$ are formulated by

$$\mathbf{M}_t = \begin{bmatrix} m_f + X_{\dot{u}} & 0 & -m_f y_c \\ 0 & m_f + Y_{\dot{v}} & m_f x_c \\ -m_f y_c & m_f x_c & I_z + N_{\dot{r}} \end{bmatrix},$$

$$\mathbf{f}_M = \begin{bmatrix} m_f x_c \dot{\phi}^2 + (m_f + X_{vr})\dot{y}\dot{\phi} - X_{uu}|\dot{x}|\dot{x} \\ m_f y_c \dot{\phi}^2 + (m_f + Y_{ur})\dot{x}\dot{\phi} - Y_{vv}|\dot{y}|\dot{y} \\ m_f x_c \dot{x}\dot{\phi} + m_f y_c \dot{y}\dot{\phi} - N_{rr}|\dot{\phi}|\dot{\phi} \end{bmatrix} \tag{23}$$

$$\mathbf{u}_I = \begin{bmatrix} u_{x,T} \\ u_{y,T} \\ u_{\phi,T} \end{bmatrix} = \begin{bmatrix} T_1 \\ T_2 + T_3 \\ l(T_2 - T_3) \end{bmatrix},$$

where the subscripts u and v mean the velocities of UWR in x and y directions respectively. Brief descriptions and corresponding nominal values of parameters in Eq.(23) are presented in Table 1. The detailed descriptions for the dynamic equation of UWR and the model parameters are presented in Ref.[11].

In (22) and (23), the total mass and resistive forces include uncertain terms. For controller design, Eq.(22) is rearranged by

$$\ddot{\mathbf{x}} = \hat{\mathbf{M}}_t^{-1}\hat{\mathbf{f}}_M(\mathbf{x},\dot{\mathbf{x}}) + \hat{\mathbf{M}}_t^{-1}\mathbf{u}_I + \boldsymbol{\eta}, \tag{24}$$

where $\boldsymbol{\eta} = (\mathbf{M}_t^{-1}\mathbf{f}_M - \hat{\mathbf{M}}_t^{-1}\hat{\mathbf{f}}_M) + (\mathbf{M}_t^{-1} - \hat{\mathbf{M}}_t^{-1})\mathbf{u}_I$. Comparing Eq.(24) with Eq.(8), $\mathbf{M}_t^{-1}\mathbf{f}_M(\hat{\mathbf{M}}_t^{-1}\hat{\mathbf{f}}_M)$ is matched to $\mathbf{f}(\hat{\mathbf{f}})$ and $\mathbf{M}_t^{-1}(\hat{\mathbf{M}}_t^{-1})$ is to $G(\hat{G})$, respectively.

With the future output error defined as $\mathbf{e}(t+h) = \mathbf{x}(t+h) - \mathbf{x}_d(t+h)$, the basic control law for the nominal system is

$$\mathbf{u}_c(t) = -(\Lambda(h)\hat{\mathbf{M}}_t^{-1})^{-1} \left[\mathbf{z}_e + \Lambda(h)\hat{\mathbf{M}}_t^{-1}\hat{\mathbf{f}}_M - \Lambda(h)\ddot{\mathbf{x}}_d(t)\right], \tag{25}$$

where $\Lambda(h) = \mathrm{diag}[h^2/2!, h^2/2!, h^2/2!]$ and $z_{e,i} = e_i + h\,\dot{e}_i$ with $e_i = x_i - x_{d,i}$.

All uncertain parameters except x_c and y_c vary in the range of

Table 1. Parameters of UWR

Parameters	Descriptions	Nominal Value
mf	Vehicle mass	41.77 Kg
Iz	Moment of inertia for z axis	1.5087 Kg · m^2
xc	Position of center of mass in x axis	0 mm
yc	Position of center of mass in y axis	0 mm
$X_{\dot{u}}$	Coeff. of hydrodynamic added mass force in x direction	7.68 Kg
$X_{\dot{v}}$	Coeff. of hydrodynamic added mass force in y direction	7.45 Kg
X_{VT}	Coeff. of hydrodynamic added mass force	7.45 Kg
Yur	Coeff. of hydrodynamic added mass force	7.68 Kg
$N_{\dot{r}}$	Coeff. of hydrodynamic added moment of inertia torque	1.251 Kg · m^2
X_{uu}	Coeff. of hydrodynamic drag force in x direction	18.24 Kg/m
Y_{VV}	Coeff. of hydrodynamic drag force in y direction	25.20 Kg/m
N_{rr}	Rotational drag coefficient	1.798 Kg/ m^2
l	Distance from the front thruster to the real thruster	836 mm

$$\alpha_i^{-1}\hat{P}_i \le P_i(t) \le \alpha_i\hat{P}_i,$$

where P_i and $\hat{P}_i$ are ith uncertain parameter and its nominal value, respectively and α_i is the extent of variation (α_is in M_t are set to 6 and α_is in $\mathbf{f}_M$ are given by 5). The x_c and y_c are varied within the range of -10~10mm. Under this condition, the bounds of modeling uncertainties can be obtained by

$$\left\|M_t^{-1}\hat{M}_t\right\| \le d_M = 0.435638,$$
$$\left\|\Sigma_M\right\| = \left\|M_t^{-1}\hat{M}_t - I_3\right\| \le \gamma_o = 0.692884,$$
$$\left\|\mathbf{f}_M - \hat{\mathbf{f}}_M\right\| \le d_F(\mathbf{x},\dot{\mathbf{x}}) = \left\| \begin{matrix} m_f\,|\Delta x_c|\dot{\phi}^2 + |\Delta X_{vr}|\,|\dot{y}\dot{\phi}| + |\Delta X_{uu}|\,\dot{x}^2 \\ m_f\,|\Delta y_c|\dot{\phi}^2 + |\Delta Y_{ur}|\,|\dot{x}\dot{\phi}| + |\Delta Y_{vv}|\,\dot{y}^2 \\ m_f\,|\Delta x_c|\,|\dot{x}\dot{\phi}| + m_f\,|\Delta y_c|\,|\dot{y}\dot{\phi}| + |\Delta N_{rr}|\,\dot{\phi}^2 \end{matrix} \right\|,$$

where Δ means the maximum deviation between the parameter and its nominal values.

The transformed robust control has the form of Eq.(14) and d_η in Eq.(13) becomes

$$d_\eta = d_F(\mathbf{x},\dot{\mathbf{x}})d_M\,\|\hat{M}_t^{-1}\| + \gamma_o\,\|\mathbf{d}_s(\mathbf{x},\dot{\mathbf{x}})\|,$$

where $\mathbf{d}_s = -\Lambda(h)^{-1}\mathbf{z}_e + \ddot{x}_d$. The robust control is $\mathbf{u}_R(t) = \hat{M}_t\mathbf{u}_R^M(t)$. The adaptive control is

$$\mathbf{u}_A^M(t) = -\int_0 \delta(\tau)^2\Gamma_S\bar{\mathbf{m}}(\tau)d\tau, \text{ and } \mathbf{u}_A(t) = \hat{M}_t\mathbf{u}_A^M(t)$$

For the simulation test, the desired trajectories for UWR are given by

$$0\le t\le 10:\ X_d(t) = R_a\cos(\phi_d(t)),$$
$$Y_d(t) = R_a\sin(\phi_d(t)),$$
$$\phi_d(t) = \pi/2 + (2\pi/T_{path})t,$$

where X_d and Y_d are the desired position in the global coordinate. The initial values of all states are set to zero. The quantity given in the global coordinate is converted into the corresponding value in the local coordinate via the transformation matrix such as

$$\begin{bmatrix} e_x \\ e_y \\ e_\phi \end{bmatrix} = \begin{bmatrix} \cos\phi & \sin\phi & 0 \\ -\sin\phi & \cos\phi & 0 \\ 0 & 0 & 1 \end{bmatrix}\begin{bmatrix} e_X \\ e_Y \\ e_\phi \end{bmatrix}.$$

Fig.4 shows the path tracking performance of this controller. In the captions of the figures, the acronym NPC represents the controller only composed of the basic control law, the acronym RNPC means the controller composed of the basic and robust controls, and the acronym ARNPC is used for indicating the controller composed of the basic, robust, and adaptive controls. In this simulations, the desired path was set by R_a = 1m

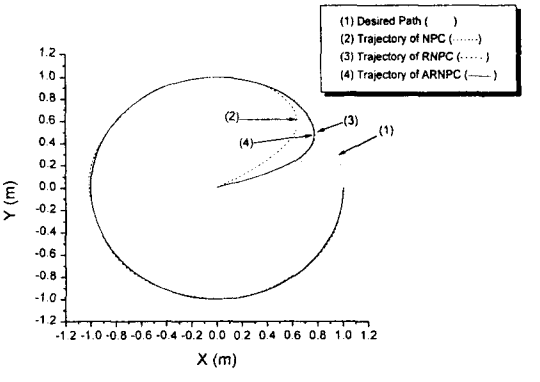

Fig. 4. Results of Circular Path Tracking of UWR

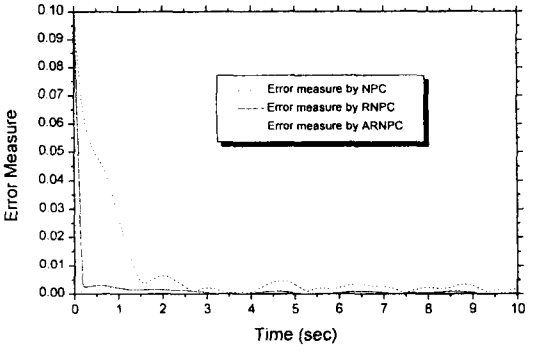

Fig. 5. Error Measures for Boundary Value ε = 0.025

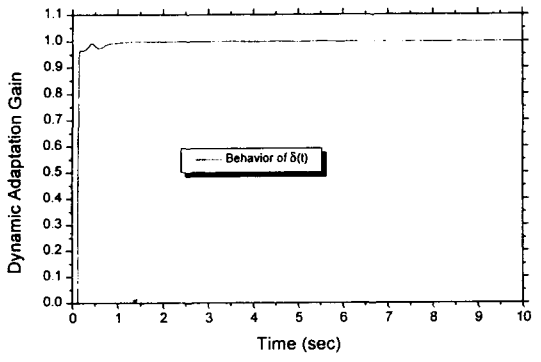

Fig. 6. Behavior of Dynamic Adaptation Gain

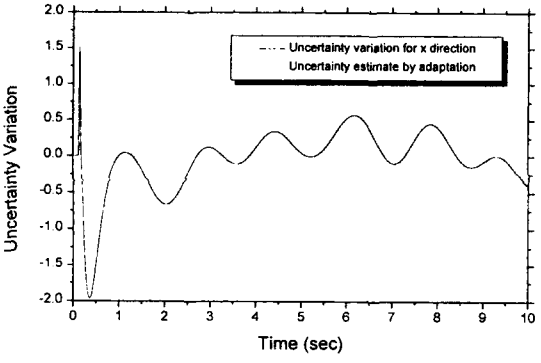

Fig. 7. Adaptive Estimation of Corresponding Uncertainty

and T_{path} = 10sec. The control instance T_c is 100msec and the prediction time interval h is given by $30 \times T_c$. The boundary value ε is 0.025, diagonal terms in static adaptation gain are given as Γ_s = diag[500,500,500], and the matrix Q is set by Q = diag[1,1,1,0.1, 0.1,0.1]. The uncertain parameters vary according to the appropriate periodic functions whose periodic dynamics are slow. Fig.5 shows the behaviors of error measures for these three controls. As can be seen in Fig.4 and Fig.5, the robust control with the adaptive control (ARNPC) shows the best control performance. The boundary value ε = 0.025 is a little bit conservative when comparing with the range of the error measure, which means the gain in the robust control is more conservative.

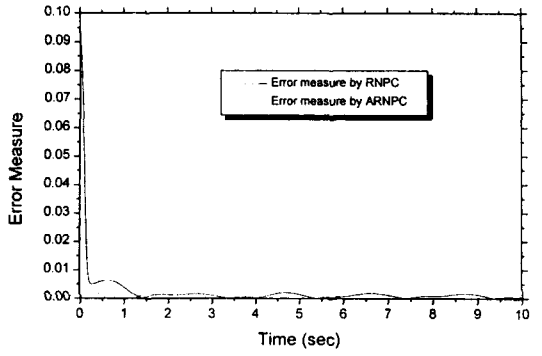

Fig. 8. Error Measures for Boundary Value ε = 0.08

Fig.6 shows the variation of the dynamic adaptation gain. From t=0 to t=0.12 sec, this value is zero because the error measure is at the outside of the boundary layer in this time interval. From t=0.12, the error measure begins to enter into the boundary layer and thus the dynamic adaptation gain gets a nonzero value. Fig.7 shows the adaptive estimation of corresponding uncertainty for x direction. The adaptive estimations of other two directions are not presented in this paper but their results are similar to Fig.7. From Fig.7, it is concluded that the adaptive control can estimate very well the corresponding uncertainty with slow dynamics. Fig.8 shows the behaviors of two error measures where, in this case, the boundary value is given by ε = 0.08. From the results in Fig.5 and Fig.8, the control performance of RNPC is deteriorated when the boundary value is increased while the control performance of ARNPC remains the same except for the initial stage within the boundary layer.

The trajectories and the error measures for sudden, unexpected disturbances are shown in

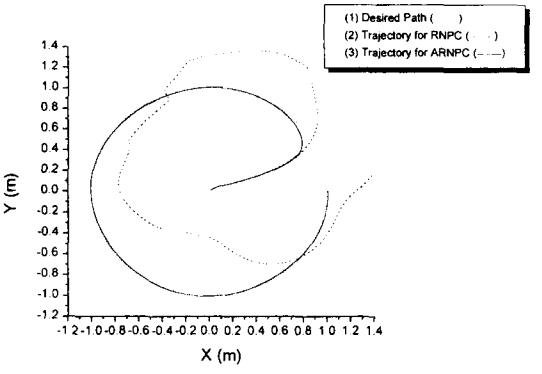

Fig. 9. Results of Circular Path Tracking for Unexpected Disturbances

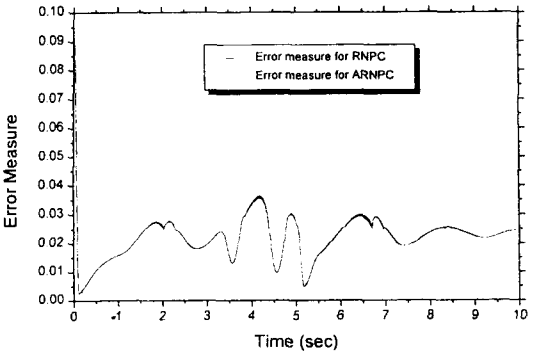

Fig. 10. Error Measures (ε=0.025) for Unexpected Disturbances

Fig.9 and Fig.10, where the disturbance of $\mathbf{d}_E^U$ = $[20, 20, 0]^T$ is applied to the system dynamics after the error measure enters into the boundary layer. From the above results, the control performance of RNPC is poor but the control performance of ARNPC shows satisfactory regardless of the unexpected disturbances. It is thought that, for RNPC, no divergence of the error measure at the outside of the boundary layer is due to the very conservative setting of the gain in the robust control. Throughout all simulation tests, the control chattering is not observed except for a case of RNPC under unexpected disturbances, though not shown in this paper.

6. Conclusions

An adaptive control is introduced into the robust control design in order to resolve the troublesome problem for selecting the appropriate boundary value and to improve the control performance within the boundary layer. The adaptive control does not compensate, independently, for the effects of the modeling uncertainties and disturbances but supports the task of the robust control in that it estimates the portion of the reverse effects that are not addressed by the robust control inside the boundary layer and compensates for this portion so that the global asymptotic stability of feedback dynamics within the boundary layer can be achieved. The nonlinear prediction model is used for developing the basic control law, which helps skipping over the selection stage of the proper hyper/sliding plane. This control method is applied to the motion control of an UWR developed for inspecting the radiation-contaminated level on the wall surfaces in the nuclear research reactor, TRIGA MARK III. From the simulation results, this controller shows satisfactory and encouraging control performance.

References

1. J. Y. Hung, W. Gao, and J. C. Hung, "Variable Structure Control: A Survey", *IEEE Trans. on Industrial Electronics*, 40, no.1, pp.2~22 (1993).
2. R. A. DeCarlo, S. H. Zak, and G. P. Matthews, "Variable Structure Control of Nonlinear Multivariable Systems: A Tutorial", *Proceedings of IEEE*, 76, no.3, pp.212~232 (1988).
3. J. J. E. Slotine and J. A. Coetsee, "Adaptive

Sliding Controller Synthesis for Nonlinear Systems", *International Journal of Control*, 43, no.6, pp.1631~1651 (1986).

4. H. Elmali and N. Olgac, "Sliding Mode Control with Perturbation Estimation (SMCPE): A New Approach", *International Journal of Control*, 56, no.4, pp.923~941 (1992).
5. P. Lu, "Optimal Predictive Control of Continuous Nonlinear Systems", *International Journal of Control*, 62, no.3, pp.633~649 (1995).
6. G. Y. Park, J. S. Yoon, and Y. S. Park, "Robust Nonlinear Predictive Control of Underwater Wall-Climbing Robot", *Institute of Control, Automation, and System Engineering*, 4, no.6, pp.772-779 (1998).
7. G. Y. Park and J. S. Yoon, "Design of an Adaptive Robust Nonlinear Predictive Controller", *Institute of Control, Automation, and System Engineering*, 7, no.12, pp.967-972 (2001).
8. J.-J. Slotine and L. Weiping, *Applied Nonlinear Control, Prentice Hall*, pp.229~230 (1991).
9. D. S. Yoo and M. J. Chung, "A Variable Structure Control with Simple Adaptation Laws for Upper Bounds on the Norm of the Uncertainties", *IEEE Trans. on Automatic Control*, 37, pp.860~865 (1992).
10. Y. S. Park, G. Y. Park, J. S. Yoon, B. J. Lee, and W. Z. Oh, "Design and Control of Underwater Wall Ranging Robot for Inspection of Research Reactor", in *Field & Service Robotics-Springer-Verlag Engineering Series*, pp.245-250, April (1998).
11. M.Y. Kim, K.H. Kim, H.S. Cho, G. Y. Park, and J. S. Yoon, "A Shallow AUV In Nuclear Power Plants: Design and Implementation," *Proc. of International Conference on Mechatronics Technology*, Taiwan, November (1998).

Appendix A: Define the Lyapunov function candidate V as

$$V = \frac{1}{2}\mathbf{e}_v^T P \mathbf{e}_v, \tag{A1}$$

where P satisfies the following Lyapunov equation: $\Gamma^T P + P\Gamma = -Q$, for $Q>0$.

By use of Eq.(11), the time derivative of V is represented as

$$\dot{V} = -\frac{1}{2}\mathbf{e}_v^T Q \mathbf{e}_v + \mathbf{e}_v^T P B_v (\mathbf{u}_R^M + \boldsymbol{\eta})$$

$$= -\frac{1}{2}\mathbf{e}_v^T Q \mathbf{e}_v + \overline{\mathbf{m}}\mathbf{u}_R^M + \overline{\mathbf{m}}\boldsymbol{\eta}$$

The time derivative of V is further manipulated, by use of Eq.(12), such that

$$\dot{V} \le -\frac{1}{2}\mathbf{e}_v^T Q \mathbf{e}_v + \overline{\mathbf{m}}\mathbf{u}_R^M + \| \overline{\mathbf{m}} \| \| \boldsymbol{\eta} \|$$

$$\le -\frac{1}{2}\mathbf{e}_v^T Q \mathbf{e}_v - (d_\eta + \xi)\| \overline{\mathbf{m}} \| + d_\eta \| \overline{\mathbf{m}} \| \tag{A2}$$

$$\le -\frac{1}{2}\mathbf{e}_v^T Q \mathbf{e}_v .$$

Since Q is positive definite, $\dot{V}$ is negative semi-definite as can be seen in (A2). Therefore, the Lyapunov function (A1) is the non-increasing function. If the initial value of Lyapunov function, V(0), is finite, then V(t) is finite for $\forall t>0$. From (A1), $\mathbf{e}_v$ is also finite for $\forall t>0$ ($\mathbf{e}_v \in L_\infty$). By examining Eq.(11), $\dot{\mathbf{e}}_v$ is finite ($\dot{\mathbf{e}}_v \in L_\infty$) for $\forall t \ge 0$ because $\mathbf{e}_v$ and other terms such as Γ_v, B_v, $\mathbf{u}_R^M$, and $\boldsymbol{\eta}$ are finite for $\forall t \ge 0$. By integrating both sides of (A2) from t=0 to t=∞, the following inequality is obtained:

$$\int_0^\infty \mathbf{e}_v(\tau)^T Q \mathbf{e}_v(\tau) d\tau \le 2\left[V(0) - V(\infty)\right] < \infty .$$

From the above result, the augmented error $\mathbf{e}_v$ is square integrable ($\mathbf{e}_v \in L_2$). The fact that $\mathbf{e}_v \in L_2 \cap L_\infty$ and $\dot{\mathbf{e}}_v \in L_\infty$ concludes, by Barbalat' s lemma [1], that $\mathbf{e}_v(t) \to 0$ as $t \to \infty$. And this means equally $\mathbf{e}(t) \to \mathbf{0}$ as $t \to \infty$. Hence, $\mathbf{y}(t) \to \mathbf{y}_d(t)$ as $t \to \infty$ can be

achieved. ■

Appendix B: Let the Lyapunov function within the boundary layer be

$$V = \frac{1}{2}\mathbf{e}_v^T P \mathbf{e}_v + \frac{1}{2}\tilde{\mathbf{d}}^T \Gamma_S^{-1} \tilde{\mathbf{d}}.$$

With Eq.(15), the time derivative of V becomes

$$\begin{aligned}
\dot{V} &= -\frac{1}{2}\mathbf{e}_v^T Q \mathbf{e}_v + \bar{\mathbf{m}}(\mathbf{u}_R^M + \mathbf{u}_A^M + \eta + \mathbf{d}_E^U) + \dot{\tilde{\mathbf{d}}}^T \Gamma_S^{-1} \tilde{\mathbf{d}}, \\
&= -\frac{1}{2}\mathbf{e}_v^T Q \mathbf{e}_v + \bar{\mathbf{m}}\mathbf{u}_R^M + \bar{\mathbf{m}}[(1-\delta(t))\eta_c + \Sigma_M \mathbf{u}_R^M] \\
&\quad + \bar{\mathbf{m}}[\delta(t)\eta_c + \mathbf{d}_E^U] + \bar{\mathbf{m}}[I_m + \Sigma_M]\mathbf{u}_A^M + \dot{\tilde{\mathbf{d}}}^T \Gamma_S^{-1} \tilde{\mathbf{d}}, \\
&= -\frac{1}{2}\mathbf{e}_v^T Q \mathbf{e}_v + \bar{\mathbf{m}}\mathbf{u}_R^M + \bar{\mathbf{m}}\left[(1-\delta(t))\eta_c + \Sigma_M \mathbf{u}_R^M\right] \\
&\quad + \bar{\mathbf{m}}\delta(t) G(\mathbf{x})\hat{G}(\mathbf{x})^{-1}\left[\eta_c^M + \delta(t)^{-1}\mathbf{u}_A^M\right] + \dot{\tilde{\mathbf{d}}}^T \Gamma_S^{-1} \tilde{\mathbf{d}}, \\
&= -\frac{1}{2}\mathbf{e}_v^T Q \mathbf{e}_v + \bar{\mathbf{m}}\mathbf{u}_R^M + \bar{\mathbf{m}}\left[(1-\delta(t))\eta_c + \Sigma_M \mathbf{u}_R^M\right] \\
&\quad + \left[\bar{\mathbf{m}}\delta(t) G(\mathbf{x})\hat{G}(\mathbf{x})^{-1} + \dot{\tilde{\mathbf{d}}}^T \Gamma_S^{-1}\right]\tilde{\mathbf{d}}.
\end{aligned} \tag{B1}$$

When Eq.(17) is applied to (B1), the terms in the bracket in the most right hand side are vanished out and the resulting time derivative of V is bounded by

$$\dot{V} \le -\frac{1}{2}\mathbf{e}_v^T Q \mathbf{e}_v + \bar{\mathbf{m}}\mathbf{u}_R^M + \left\|\bar{\mathbf{m}}[(1-\delta(t))\eta_c + \Sigma_M \mathbf{u}_R^M]\right\|. \tag{B2}$$

By applying Eq.(14) and Eq.(18) to (B2), (B2) can be further rearranged into

$$\begin{aligned}
\dot{V} &\le -\frac{1}{2}\mathbf{e}_v^T Q \mathbf{e}_v - (1-\gamma)\, d_{max}\frac{\|\bar{\mathbf{m}}\|^2}{\varepsilon} + \|\eta_c\|\frac{\|\bar{\mathbf{m}}\|^2}{\varepsilon} \\
&\le -\frac{1}{2}\mathbf{e}_v^T Q \mathbf{e}_v.
\end{aligned} \tag{B3}$$

From the results in Appendix A, (B3) produces $\mathbf{y}(t) \to \mathbf{y}_d(t)$ as $t \to \infty$. Therefore, asymptotic output tracking can be achieved for the feedback system inside the boundary layer.

Reference

1. M. Popov, *Hyperstability of Control Systems* (New York: Springer-Verlag), (1973).